Fusion as Electric Propulsion

By R.W. Bussard, Energy/Matter Conversion Corporation,
680 Garcia Street, Santa Fe, NM 87505, <emc2qed@comcast.net>

Abstract

Fusion rocket engines are analyzed as electric propulsion systems, with propulsion thrust-power-to-input-power ratio (the thrust-power "gain," G_L) much greater than unity. Gain values of conventional (solar, fission) electric propulsion systems are always quite small (e.g., $G_L < 0.8$). With these, "high-thrust" interplanetary flight is not possible, because their system acceleration (a_t) capabilities are always less than the local gravitational acceleration. In contrast, gain values 50-100 times higher are found for some fusion concepts, which offer "high-thrust" flight capability. One performance example shows a 53.3 day (34.4 powered; 18.9 coast), one-way transit time with 19% payload for a single-stage Earth/Mars vehicle. Another shows the potential for high- acceleration ($a_L = 0.55\,g_o$) flight in Earth/moon space.

Nomenclature

A_{rad} = area of waste heat radiator (one side)

a_1 = coefficient in I_{sp} equation [see Eq. (11)]

a_f = vehicle final-flight acceleration

a_{fes} = fusion-electric-engine specific mass per unit fusion power

a_o = vehicle initial-force acceleration

a_{rad} = waste-heat radiator mass per unit area (one side)

a_L = propulsion system force acceleration, F/M_{fes}

b_{ij} = radiating area factor (1 for one-sided; 2 for two-sided)

D = propellant/fuel dilution ratio, $= m_d/m_f$

F = fusion-engine net thrust

f_Q = recirculating electrical-power fraction

f_r = fusion power fraction radiated directly to space or regeneratively cooled

f_L = power fraction rejected directly to or absorbed in radiators

G_e = fusion system electric gain, $= 1/f_q = P_e/P_d$

G_f = fusion source power gain $= P_f / P_d$

g_o = gravitational acceleration at sea level

G_L = fusion propulsion power gain $= P_L / P_d$

I_{sp} = propellant/diluent specific impulse

I_{spf} = specific impulse at end of flight

I_{spm} = specific impulse at flight midpoint

I_{spo} = initial specific impulse

K_f = propulsion-system specific mass per unit fusion power $= M_L / P_f$

M_b = "burnt" mass of space vehicle $= M_o - M_p$

M_{fes} = mass of fusion electric engine system

M_L = payload mass

M_o = gross mass of space vehicle

M_p = propellant mass

M_{rad} = waste-heat radiator mass

M_{st} = miscellaneous structure and propellant tank mass

M_L = mass of fusion propulsion system $= M_{fes} = M_{rad}$

m_d = propellant diluent mass flow rate (Figure 3)

m_f = fusion-fuel mass flow rate (Figure 3)

n_c = thermal-electrical conversion efficiency

P_d = fusion system electric drive power $= f_q P_e$

P_e = fusion system gross electric power output

P_f = gross fusion power

P_r = radiated power

P_{reg} = regenerative cooling power

P_L = propulsive thrust power

T_r = waste-heat radiator temperature

T_{reg} = maximum regenerative cooling temperature

v = vehicle velocity (speed)

v_c = vehicle "characteristic" velocity

v_m = vehicle velocity at flight midpoint

ε = radiator surface emissivity

σ   = Stefan-Boltzmann radiation constant

Introduction

Analysis of low-thrust advanced propulsion systems in space flight shows that performance is strongly determined by the product of vehicle initial-force acceleration capability (a_o, the ratio of system initial thrust to vehicle initial gross mass), propellant exhaust specific impulse (I_{sp}), and engine system specific mass per unit thrust power ($K_f P_f/P_L$, including the mass of any fixed waste-heat radiators required by the engine system).

Study of Earth-moon and interplanetary flight scenarios shows that efficient system performance requires values of this product that allow vehicle operation as a "high-thrust" system during its powered flight within the local gravity field. This is readily seen in Figure 1, by Hunter,[1] which shows the velocity increment required for orbital flight to a range of final velocities, as a function of vehicle acceleration. The figure plots the ratio of total velocity change to initial circular (orbital) velocity of a space vehicle transferring from initial circular orbital speed in a gravitational field of local strength g to a range of final speeds beyond escape velocity from the initial orbit. Curves are shown for this "hyperbolic excess velocity" ranging from zero (barely reaches escape speed) to 1.5 (escapes the gravitational system with speed excess 1.5 times initial orbital speed).
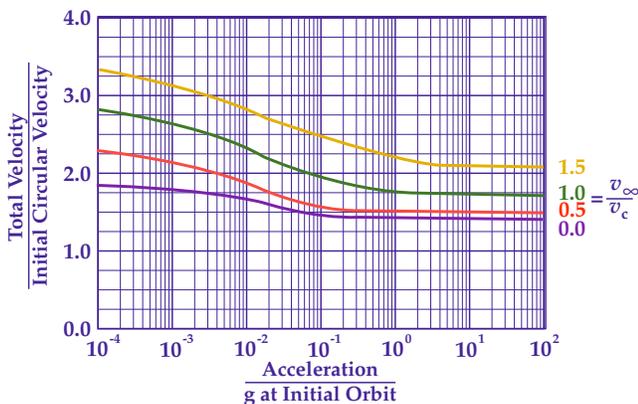

Figure 1 — Rocket vehicle "characteristic" velocity requirements vs propulsion-system acceleration for various hyperbolic excess velocities. [1]

The most striking feature of these curves is that operation at small ratios of vehicle acceleration to initial orbital gravity (i.e., at "low-thrust" conditions) requires rapidly increasing vehicle characteristic velocity increments as the hyperbolic excess speed is made larger than that for simple escape flight. In consequence, for a given mass ratio vehicle system, the I_{sp} needed at "low-thrust" will be increasingly larger than that for "high-thrust" vehicles with higher excess escape speeds. Thus, it is clear that "low-thrust" propulsion systems must produce very much higher I_{sp} exhaust streams than "high-thrust,"

if they are to compete for fast transit interplanetary flights. In a recent study, Garrison and Stocky[2] show this effect for low Earth orbit to geosynchronous Earth orbit transfers with zero hyperbolic excess velocity, based on earlier work of Etheridge.[3]

The reason for this behavior is easy to understand from elementary considerations of the expenditure of energy by the propulsion system as it climbs out of the initial gravity well. If all of the velocity increment needed to escape the gravity well is added in a short time, at the bottom of the well, no energy is expended in lifting the mass of propellant to be exhausted through a vertical rise in the gravity field. In contrast, if the velocity increment is added only very slowly, as the vehicle spirals out and up (at small force acceleration) through the gravity well, a large fraction of the total energy used is spent lifting this propellant "uphill" in the well. In the second ("low-thrust") case, therefore, considerable energy and propellant mass to absorb it must be provided simply to lift the propellant in the gravity field. This situation worsens as the desired vehicle hyperbolic excess speed is increased beyond that minimally needed for simple vehicle escape from the field, because more propellant mass is needed for higher final vehicle speed. High-thrust systems exhaust most of their propellant near the well bottom, whereas low-thrust systems pay this continuing penalty throughout their powered flight.

Of course, in a power-limited or fixed-power situation (as is the case for nearly all electric propulsion systems) the need for higher I_{sp} in "low-thrust" propulsion systems is antithetical to the very nature of the parametric variation of propulsion-system specific mass, which most often scales inversely with exhaust I_{sp} as discussed by Bussard and DeLauer.[4] Indeed, for any given propulsion system power and mass, there will always be an "optimum" specific impulse that yields the minimum-mass vehicle system for a given flight. For flights with large "characteristic velocity," conventional electric propulsion systems always optimize well on the "low-thrust" side of the flight performance curves of Figure 1. This sort of optimization is explored in more detail by Auweter-Kurtz et al.,[5] who showed this result for a range of transfer missions and thruster types.
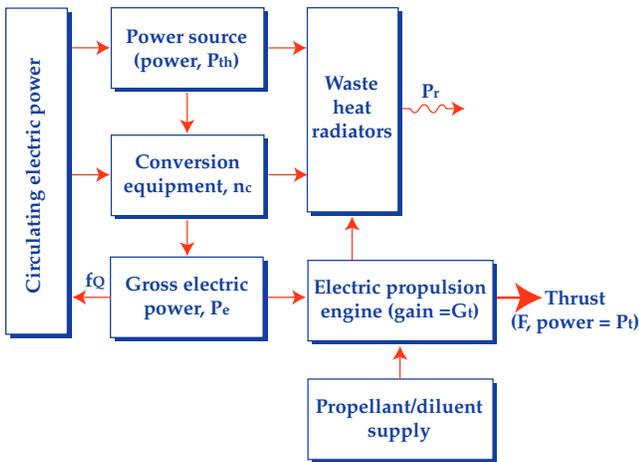
Figure 2 — Electric-propulsion system block diagram

These arguments apply to all orbital transfer flights. For operation in Earth-moon space this requires that $a_o >$ 0.03-0.3 g_o, depending on the desired hyperbolic excess velocity, whereas vehicle flight in the solar field requires only about 0.001 of these values. If 25% of the vehicle mass is allotted to the propulsion system, this must have a thrust-to-mass ratio (a propulsion system force acceleration) at least four times larger than that required for the vehicle; $(a_L/g_o) >$ 0.12-1.2 x 10^{-3} for interplanetary flight, and >0.12-1.2 for cislunar flight. Small as these limits are, they are formidable when applied to propulsion systems whose I_{sp} values are above 3000 s.

Conventional nuclear-fission-reactor electric propulsion systems exhibit $a_L <$ $10^{-4} g_o$, and can require up to 1.6-2.0 times the vehicle "characteristic" velocity capability for interplanetary operation than high-thrust vehicles, for the same flight performance, depending on the interorbital mission requirements and hyperbolic excess speed desired. This effectively nullifies some of the two- or threefold increase in I_{sp} available with such electric engine systems over competing low-I_{sp} high-thrust propulsion systems. Still higher I_{sp} values must be produced to reach flight performance superior to the high-thrust competition.

Discussion

The application of advanced (conceptual) fusion power sources to propulsion offers a new way around this dilemma. All such fusion reactors require electrical power for their operation. They act as (time-averaged) power amplifiers in the transformation of this power to output power delivered to the propellant. The output power is always greater than the input electrical drive. Thus, these reactors can be viewed as sub-system portions of complete electric propulsion systems in which the source power to drive the reactor is supplied to an "engine system" (which includes the fusion reactor) whose thrust power gain is above unity ($G_L > 1$). This is in strik-

ing contrast to conventional electric thrusters whose thrust-power gain is always[2] $G_L < 1$. Analysis of flight performance then can be made as for conventional electric propulsion systems, whether the fusion reactor unit supplies thermal or electrical energy to the thrust-producing device in the engine system.

Figure 2 shows a block diagram of a typical generalized electric propulsion system, in which separately generated electrical power is supplied to an independent electric thruster. This could apply to a fusion-electric power source driving any electric engine. The I_{sp} of propellant from such a system is bounded only by thermal loads on, and temperature limits of the engine structure, and by the fraction of fusion power deposited in this structure which is not radiated away but is absorbed by regenerative cooling of the inflowing propellant fluid. Note that the propulsion system, as defined here, includes all of the hardware components required for thrust generation. The propellant/diluent supply system can be treated separately from the other elements, and attention will be limited to these.
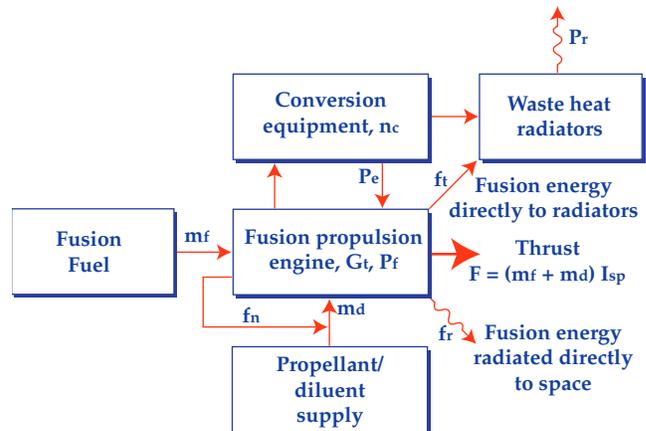

Figure 3 — Fusion propulsion as electric propulsion

Figure 3 shows a block diagram of a fusion propulsion system in which the reactor generates hot plasma that is extracted and mixed with a propellant/diluent to provide the exhaust fluid. This system must generate only enough electricity to run itself; all of its propellant heating is by thermal means. The I_{sp} is adjustable by variation of the plasma/diluent mixing or "dilution" ratio. This ratio will be in the range of $10^3 < D < 10^4$ for most systems of interest. The performance of all fusion-electric systems is also limited by materials temperature limits and radiatively absorbed power and by the mass of equipment required for waste-heat rejection and electrical power generation.

Fusion System Performance

Conventional fusion reactor designs give systems that are all very large in size (see e.g., Gross[6]) due to the low power densities inherent in their operating conditions and requirements. Study of the application of these to space propulsion shows that they are quite unpromising for most missions of interest (e.g., manned interplanetary flight, cislunar flight); their great size, mass, and nuclear radiation hazard renders them wholly noncompetitive with even the most simple chemical rocket propulsion systems.

In contrast, several concepts for advanced fusion propulsion systems show prospects for useful performance leading to greatly improved vehicle flight capabilities, as compared with conventional concepts for electric propulsion systems. These are discussed further in the following section. This potential performance advantage arises precisely because of the prospect of a gain of 50-100 times in G_L from use of such fusion systems. This will be reflected in a like reduction in the specific mass K_f of the propulsion system which, in turn, will yield a similar increase in the vehicle force acceleration capability. To see this, it is useful to examine the relations between system masses and powers for such systems.

The propulsion system mass is that of the fusion electric engine system plus that of the waste-heat radiators required, thus:

$$M_t = M_{fes} + M_{rad} \quad (1)$$

with

$$M_{fes} = a_{fes} P_f \quad (2)$$

and

$$M_{rad} = a_{rad} A_{rad} \quad (3a)$$

$$A_{rad} = \frac{P_r}{\sigma \varepsilon T_r^4 b_{ij}} \quad (3b)$$

The radiated power is related to the fusion power by a number of efficiency and leakage factors:

$$P_r = P_f[(1 - n_c)(1 - f_r - f_t) + f_t] \quad (4)$$

The propulsion system mass can now be written as:

$$M_t = (K_f)P_f \quad (5)$$

where the specific mass is found by combination of Equations. (1-4). System thrust is related to the fusion power by:

$$F = \frac{2G_t f_Q n_c (1 - f_r - f_t)P_f}{g_0 I_{sp}} \quad (6)$$

The propulsion system force acceleration is then given by the ratio of thrust (Eq. 6) to mass (Eq. 5) in which the fusion power term cancels; thus,

$$a_t = \frac{2G_t f_Q n_c (1 - f_r - f_t)}{\{g_o I_{sp}\}\left\{a_{fes} + \left[\dfrac{a_{rad}}{\sigma \varepsilon T_r^4 b_{ij}}\right][(1 - n_c)(1 - f_r - f_t) + f_t]\right\}} \quad (7)$$

From this, it is evident that large I_{sp} will yield small acceleration unless thrust-power gain is high and engine system and radiator specific masses are low. In most conventional electric propulsion systems, gain is only $0.5 < G_L < 0.8$ and engine system specific mass is $a_{fes} > 5$ kg/kW. With reasonable values of the other parameters, Eq. (7) shows that the force acceleration of such systems typically is only $a_L < 10^{-4} g_o$. As in Figure 1, this is "low-thrust" performance, resulting in demands for higher I_{sp} to overcome the deleterious effect of the low acceleration of the vehicle.

Potential Fusion Propulsion Systems

In contrast, an advanced fusion system with $G_L = 30$, for example, and an engine specific mass of only $a_{fes} = 5.0 \times 10^{-2}$ kg/kW could yield $a_L = 1.7 \times 10^{-3} g_o$ for $I_{sp} = 6000$ s if the radiator mass were three times the reactor-electric system mass. Such a performance level would put fusion flight in the "high-thrust" regime for interplanetary missions, even for this low level of vehicle acceleration. This, in turn, yields vehicle "characteristic" velocity capability 1.4 times larger for Hohmann orbits and over 2 times larger for fast transits than for conventional systems of the same mass ratio. Such fusion-system performance thus would offer consequent great reduction in flight times or increase in payload fractions from other electric propulsion systems. It is a happy accident of nature that concepts do exist for fusion systems of such performance, which neatly fall well on the "high-thrust" side of the space flight-performance curves.

Compact Tokamak Magnetic Confinement Fusion Reactors

An example of this type of fusion propulsion system for interplanetary flight is illustrated in Figs. 4 and 5. These show a cross section through a compact high-field tokamak[7] capable of operating on the deuterium (DD) fusion reaction process (or, alternatively, on the D³He cycle) and its assembly into a rocket engine thrust system.

This machine is designed so as to allow escape of hot plasma from the reacting core region, through magnetic "divertor" nozzles around the outer periphery of the slots between conductor turns of the toroidal magnet

coil system. Plasma at temperature of the order of 10-40 keV is extracted at a pressure of about 30 atmosphere (ca. 2-4% plasma "beta") and mixed with the propellant/diluent stream external to the reactor, as shown in Figure 5. The mixed flow (nearly all diluent) is then exhausted through a converging-diverging nozzle to provide high-I_{sp} thrust. The divertor-mixer chamber and nozzle walls are insulated by surface magnetic fields generated by current flowing in conductors wound on the structure exterior surfaces. Such "magnetic insulation" can give reductions in surface heat transfer by factors of 20-200 from that for simple forced convection alone.

This device thus heats propellant by thermal mixing with superhot plasma from fusion reactions; no electrical heating is involved. The only electrical power needed is that required to drive the tokamak itself. This power is provided by a turbine-generator system driven by a low-temperature Rankine steam cycle. The schematic drawing in Figure 5 shows the turbine-generator system mounted forward of the reactor and shielded against neutron radiation by a shadow shield covering about 0.1 spheradians (approximately 100-degree cone angle). Steam is generated by passing condensate feed water through the toroidal magnet coils, the reactor interior wall, and other reactor internal and support structures requiring cooling. Some electrical power is used to drive the feed-water pumps and some for the propellant pumps. The propellant is pumped first to the shield to extract its thermal source load, and then to the mixer-divertor chambers around the reactor plasma extraction region. Further details of the system design concept are given later.

The DD reaction has two branches of equal probability, each of which produces additional fusion fuels (tritium, T, and helium-3, ^{3}He); thus:

$$D + D \therefore T (1.01 \text{ MeV}) + p(3.02 \text{ MeV}) \quad (8a)$$

$$D + D \therefore {}^3\text{He} (0.82 \text{ MeV}) + n(2.45 \text{ MeV}) \quad (8b)$$

where n and p denote neutrons and protons, respectively. In thermonuclear reactors these fuels may also undergo fusion with the D present according to:

$$D + T \therefore {}^4\text{He}(3.5 \text{ MeV}) + n(14.1 \text{ MeV}) \quad (9)$$

$$D + {}^3\text{He} \therefore {}^4\text{He}(3.6 \text{ MeV}) + p(14.7 \text{ MeV}) \quad (10)$$

If all of the secondary fuels are burned, 0.617 of the total energy is produced in charged particles with 0.383 carried by neutrons. If none of the secondary fuels are burned, 0.664 energy fraction is in charged particles with 0.336 in neutrons. Since thrust is produced by mixing hot plasma with cold diluent/propellant, it is certain that some of the unburned secondary fuel nuclei will be swept out into the propellant stream. For purposes of calculation, it is assumed that about 50% of these fuels

are burned, leading to an energy distribution of 0.64 in charged particles and 0.36 in neutrons.

Neutron energy is generally unusable in propulsion systems of the type considered here, as the neutrons carry their energy away from source plasma and deposit it in any material with which they collide. This creates both an energy-loss mechanism and a structure cooling problem. In general, the DD reactions are more difficult to achieve than is the D + T (tritium) fusion reaction alone, but they yield more energy in charged particles and less in neutrons. Note that the D^{3}He reaction yields only charged particles and, thus, is more desirable from these points of view.

The reactor shown (Figure 4) is derived from the Riggatron tokamak,[8] which used water-cooled copper alloy toroidal magnet field coils capable of producing central toroidal fields up to 20 T (200 kG). The torus major radius is 1.6 m and its minor radius is 0.8 m with a 1.5:1 elongation of the plasma cross section. Assuming copper alloy toroidal coils whose thickness varies from 10 cm at outside to 20 cm at inside positions, the reactor mass is estimated to be approximately 7.0x 10^4 kg.
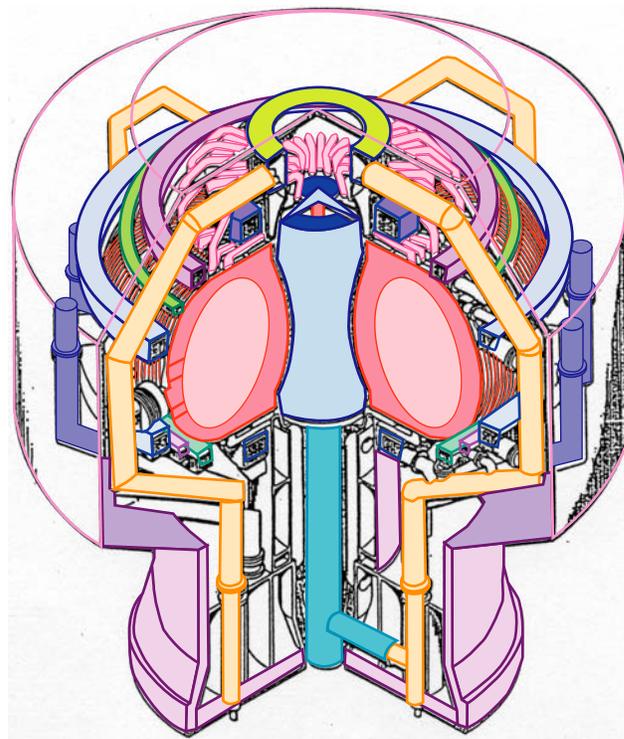

Figure 4 — Compact DD (or D^{3}He) tokamak fusion reactor

Detailed computer calculations of fusion ignition, by Wagner,[9] extended to DD and D^{3}He fusion, showed the ability of the device to ignite with an initial DT charge, "bootstrap" to high temperature, and switch over to DD and/or D^{3}He for full power burn. The model chosen here is based on DD fusion simply because ^{3}He is so rare on Earth. As pointed out by Wittenberg et al.,[10] sources of ^{3}He on the moon (trapped in lunar surface dust and

rocks) may be very large and suffice to fuel a future fusion rocket (and power) economy, but they are not yet available.

This size of reactor is a minimal practical size for ready achievement of fusion ignition and burn of DD. For this, the nominal DD reaction power is taken as 6630 MW (fusion), about the maximum that can be handled with realistic heat-transfer cooling means and designs in this size of machine. The neutron power is 2387 MW(n), of which 20% is intercepted by structure. The charged particle power is 4243 MW(cp) and 7.5% of this (318 MW) is assumed to be incident on the reactor liner/wall. This leaves 92.5% of the charged particle power (3925 MWth) for use to heat propellant/diluent. The captured neutron power of 477 MW is split between 30 MW deposited in the shadow shield and 447 MW in the reactor first wall and magnet coil material.

In order to ignite and drive the tokamak, electrical power must be supplied to its drive and toroidal field coils. Averaged over a power cycle, the power required is 200 MWe. In addition to this electrical demand, the pumps for steam cycle feed water and, for LH_2 propellant/diluent, require an additional 16 MWe and 5 MWe, respectively. Thus, 221 MWe must be generated. With this output gross electrical power, the fusion-power-to-electrical-power gain is G_f = 6630/221= 30.0. and the system thrust-power-to-electrical-power gain is G_L = 3926/221 = 17.8.

The feed-water pump power appears in the steam cycle as a thermal input, whereas the LH_2 pump acts to heat the diluent inflow stream. And all of the electrical power driving reactor coils appears as ohmic resistive heating, which must be removed by the water cooling flow. The total thermal waste-heat load on the radiator is thus the sum of the reactor-structure-deposited heat power, the electrical drive power, and the water pump power. This is 996 MWth, which must be radiated to space.
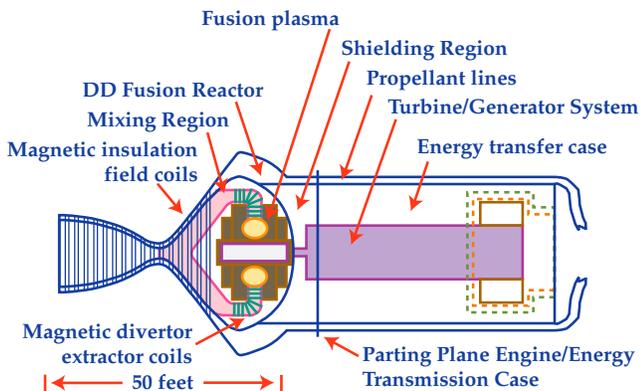

Figure 5 — DD fusion rocket engine system

The diluent inflow is used to cool the shadow shield and thus must absorb the deposited power as well as that of the LH_2 pump. Using the values cited above, the total

LH_2 pre-heat power will be 35 MWth. If the shield material is constrained to operate at or below 1900 K, the regenerative cooling limit on specific impulse will be I_{sp} = 7570 s. Nozzle cooling can be accomplished easily by use of bypass diluent, heated to the wall-limiting temperature, and exhausted to space for attitude control or minor additional thrust. Assuming the wall cooling load fraction to be 0.01 of the propellant power throughflow, and a wall limit of 1400 K, the bypass I_{sp} would be about 430 s. Ignoring this low value (compared to main engine), the bulk average limiting specific impulse would be I_{sp} = 7420s.

The steam cycle is chosen to fit the temperature limitations of materials in the reactor, while preserving a conventional thermal conversion cycle. If high-strength copper alloys are used[8] for the toroidal coils, it is possible to operate them in their least stressed (outer) sections at temperatures up to 700°F. If necessary, since neutron conservation is not needed (as for T-breeding in DT tokamaks), tungsten fiber reinforcement can be employed in the coil material as well, and/or steel loading bands can be added for strength.

At this temperature, a desirable pressure for some degree of superheat in the steam is 1470 psia (100 atm). Expansion from this temperature can be made through a high-pressure turbine of modest expansion ratio, to conditions chosen for the bottom of the turbine cycle, at 470 psia pressure and 460°F temperature. This requires use of a condensing turbine with about 11.5% condensation in the turbine exhaust. With these conditions, the overall thermal conversion cycle efficiency is only 221/996 = 0.222. Note that the electrical power produced is only 0.0333 (= $1/G_e$) of the gross fusion power.

The waste-heat radiator will operate at or just below the turbine exhaust temperature of 460°F and the maximum pressure of 31.5 atmosphere, rejecting 996 MWth of thermal power to space. Using a cruciform radiator configuration with four flat panels extending the length of the spacecraft (as shown in Figure 6), the radiator effectiveness will be reduced by thermal blocking due to adjacent panels. Accounting for this effect for a cosinusoidal angular distribution of surface radiation, the effective emissivity is taken to be ε =0.8. With this, the radiating area (both sides) required is 3.669 x 10^6 ft². This is composed of an array of 21 x 21 modular panels, each 20 ft x 52 ft in size.
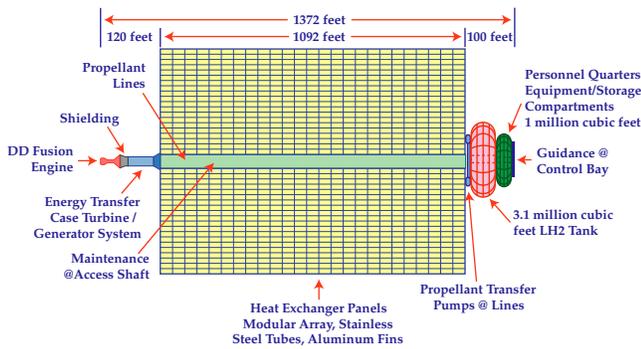
Figure 6 — DD Fusion Interplanetary Spacecraft

Each modular unit is formed from aluminum sheet fins, with radial stainless steel tubes of 0.125 inch inside diameter at a spacing of 0.333 ft across the module length. Thus, there are 156 coolant tubes, 20-ft long in each module. The aluminum fins have a mean thickness of 0.060 inch, varying from 0.120 inch at the tube positions to near-zero at the midpoint between tubes, giving a fin temperature drop of 46°F. Pressure drop in tube flow over the 20-ft module height is only about 40 psi at a flow speed of 13 feet/sec. This is partially compensated by spacecraft rotation at 5 rpm, to give one gravity (approximately) at 100-ft radius. The total mass of the radiator system including tubes, headers, fins, and condensate is estimated to be 7.6×10^5 kg. The specific mass required is 4.46 kg/m² or 0.913 lb/ft², well within normal conventional technical capabilities.

This minimum practical size for the DD tokamak operates optimally at the general level of power cited above. This power level, in turn, leads to a maximum thrust level for any given I_{sp} and, thus, to a minimum size and mass for the space vehicle to be driven by this engine. Figure 6 shows an outline drawing of such a spacecraft with a gross mass at launch of $M_o = 1.0 \times 10^7$ kg (10,000 metric tons). This quarter-mile-long vehicle must be launched from solar orbit (at the Earth's orbit, $g_{sol} = 0.606 \times 10^{-3} g_o = 0.0195$ ft/sec²), as its engine system is not "high-thrust" in the Earth's gravity field.

Consider a flight with an initial acceleration phase and a final deceleration phase of equal velocity increment. For a spacecraft with mass ratio such that $LN(M_o/M_b) = 1$, the total propellant fraction will be just 0.631 of the gross initial mass. At the start of powered flight, the thrust level should be taken as high as possible to reduce "gravity losses" in the local gravitational field, but the I_{sp} should be increased throughout the flight to achieve the highest possible vehicle characteristic velocity (v_c) capability. The actual speed history will be determined by the I_{sp} variation and by the interorbital transfer mission chosen for study. An optimum variation exists for any given mission [4,5]; however, here it is sufficient to examine a simple linear variation of I_{sp} during flight in free space. This variation with flight speed gives the relation $I_{sp} = I_{spo}[1 + a_1(v/v_c)]$, where the coefficient is determined

by specification of initial and final I_{sp}. With this, a momentum balance gives the mass-ratio equation as:

$$[v_c][LN\left(\frac{I_{spf}}{I_{sp0}}\right)] = \left[\left(\frac{I_{spf}}{I_{sp0}}\right) - 1\right][g_0 I_{sp0}]\left[LN\left(\frac{M_0}{M_b}\right)\right]$$

(11)

where the final speed at propellant exhaustion would be v_c in continuously accelerated flight. For the acceleration / deceleration model chosen, the speed at midpoint will be just $v_m = v_c/2$. For any given initial and final values and variation of I_{sp}, the vehicle velocity increment capability thus can be determined from Eq. 11. Here these are taken to be $I_{spo} = 5235$ s and $I_{spf} = 7365$ s, so that $I_{spm} = 6300$ s at flight midpoint. For the specified mass ratio, this gives the characteristic velocity as $v_c = 200,700$ feet/sec; thus the speed at midpoint would be 100,350 feet/sec. From these values, it is possible to calculate the propellant consumption in both phases of flight.

Now, it can be shown [e.g., Eq. 6] that the thrust is related to the I_{sp} and thrust power P_L by $F(t) = 2.0 \times 10^4 [P_L/I_{sp}(t)]$, for thrust in kilograms, with P_L in megawatts, and $I_{sp}(t)$ in seconds. With this, the propellant consumption can be determined as a function of time, and the acceleration can be found and integrated to obtain the flight speed and distance history.

Analysis of flight performance for this single-stage system shows that the initial acceleration capability is $a_o = 1.50 \times 10^{-3} g_o$, which is "high-thrust" in the solar field. The final acceleration at end of the deceleration phase is also "high-thrust," $a_f = 2.89 \times 10^{-3} g_o$. The acceleration phase of powered flight requires continuous thrust for 20.0 days, and the deceleration phase takes only 14.4 days. The distance traversed in free space during these periods would be 15.5×10^6 and 11.3×10^6 miles, respectively.

If this vehicle were launched outbound to Mars from Earth's solar orbit, it would reach its midpoint burnout condition at a position approximately 11.0×10^6 miles "down-range" (along Earth's orbit track) and 11.0×10^6 miles radially outward from its launch point. Its velocity vector would then be at an angle of about 60 degrees to the orbit tangent, and its coasting flight outward would very nearly follow this track until it reached within 8.0×10^6 miles of the Martian orbit. Assuming the Martian orbit is 50.0×10^6 miles from the Earth solar orbit, coasting flight at an average speed of 97,000 feet/sec would require 18.9 days, and the vehicle would move another 26.0×10^6 miles out and 13.0×10^6 miles downrange. The (final) deceleration phase would transport the spacecraft an additional 8.0×10^6 miles outward and downrange. The entire flight would require only about 53.3 days.

The total system mass must include that for tankage and supporting structure (M_{st}). Taking the tankage factor to be 0.09 of its contained propellant, and, allowing 0.06 of the vehicle empty mass for structure, this becomes M_{st} = 0.79 x 10^6 kg. The mass distribution is then as follows:

M_o = 10.0 x 10^6 kg

M_p = 6.31 x 10^6 kg

M_{st} = 0.79 x 10^6 kg (0.57 x 10^6 kg for tanks; 0.22 x 10^6 kg for structure)

M_L = 1.0 x 10^6 kg (0.07 x 10^6 kg for reactor; 0.17 x 10^6 for turbine generators; 0.76 x 10^6 kg for radiators)

The remaining mass of M_L = 1.90 x 10^6 kg is available for useful payload. Figure 7 summarizes these and other details of the mass distribution and flight performance of this example of a compact tokamak fusion propulsion system.

The use of D3He would yield even better performance, since the neutron production from such a fuel combination could be reduced by a factor of about 10 from that of DD. This results in a larger fraction of total fusion power available for thrust application, and a smaller fractional heat loading on the system structure. Typically, the thrust fraction is found to increase by about 1.5 times (approaching 0.9) and the radiated heat load to be reduced by about 3 times. Although the reactor mass will not change significantly, these will lead to a reduction in the waste-heat radiator mass of greater than 4 times. This mass saving can be put into payload, or into propellant which will yield higher flight speeds and shorter transit times.

Figure 7 — Performance summary: DD fusion spacecraft Earth/Mars flight

M_o = 10.00 x 10^6 kg
M_p = 6.31 x 10^6 kg
M_{st} = 0.79 x 10^6 kg
M_L = 1.9 x 10^6 kg
M_t = 1.00 x 10^6 kg (0.07 M_{reac}, 0.17 $M_{turb\text{-}elec}$, 0.76 M_{radr})

P_{fus} = 6630 MW (P_{cp} = 4243 MW, P_L = 3925 MW, P_{nL} = 2387 MW, P_{rad} = 996 MW), P_{elec} = 221 Mwe
G_f = 30.0, G_L = 17.8

I_{sp} = 5235-7365 s varying linearly with vehicle speed v

v_c = 200,700 ft/s = 38.01 miles/s
F(kg) = 2.0 x 10^4 P_L(MW)/I_{sp}(s)
F_o = 1.50 x 10^4 kg
a_o = 1.5 x 10^{-3} g_o
a_f = 2.29 x 10^{-3} g_o

Acceleration	Coast	Deceleration	Total Flight
$tb1$ = 20.0 days	$tc12$ = 18.9 days	$tb2$ = 14.4 days	53.3 days
$\Delta S1$ = 15.5 x 10^6 miles	$\Delta S12$ = 30.0 x 10^6 miles	$\Delta S2$ = 11.3 x 10^6 miles	$\Delta S1$ = 56.8 x 10^6 miles

Electrostatic Fusion Propulsion Systems

One more example serves to illustrate even greater prospects for fusion-electric rocket performance. Here the system considered is made to operate on a fusion reaction process that has no neutron yield. Several such processes exist. Among the most favorable is that using hydrogen (p) and boron-11 (^{11}B), while another of considerably greater difficulty uses (p) and lithium-7 (^{7}Li). These reactions proceed according to:

$$p + {}^{11}B \rightarrow 3\ {}^4He\ (8.7\ MeV)\quad (12a)$$

and

$$p + {}^7Li \rightarrow 2\ {}^4He\ (17.5\ Mev)\quad (12b)$$
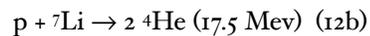
If such reactions can be maintained stably in compact devices, their output power in charged particles can, in principle, be converted directly into electric power by causing the fusion products to expand against an electric field. Suppose these reactions are made to occur at the center of a spherical electrostatic potential well, as described by Elmore et al [11] and Hirsch.[12] Charged particle products from reactions taking place within the potential well must then escape radially from the center of this sphere. Their kinetic energy can be converted directly into current flow in a spherical shell grid structure of opposing potential gradient which surrounds the potential well region. The principle of operation of this electrostatic-inertial fusion reaction device is indicated in Figure 8.

Reaction Products

Electric Potential Well

Ion Density

Voltage

-200 keV (typical)

① Deep negative electric potential well
② Traps positive ion fuels
③ In spherical radial oscillation
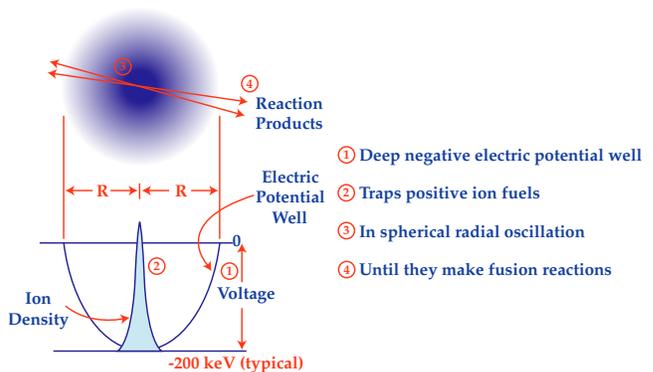④ Until they make fusion reactions

Figure 8 — General principles of electrostatic confinement fusion.

The general feasibility of direct conversion by this means has been proven by Moir and Barr in earlier research studies.[13] [14] Figure 9 shows a schematic diagram of such a direct conversion system around a spherical potential well reaction chamber. Output power from this fusion source of charged particles will be in the form of modest currents (kiloamps) at high voltages (100-1000 keV). This is suitable for direct application to the generation of low-energy relativistic electron beams (REB). The energy carried by such beams can be deposited directly, essentially completely, into rotationally-confined, magnetically-insulated, high-pressure plasmas, to produce very high gas/plasma temperatures. The resulting super-energetic plasma can be exhausted through a magnetically insulated converging-diverging nozzle to produce thrust at high I_{sp}. Operation at high chamber pressure is desirable to enhance recombination of dissociated and ionized species in the nozzle flow.

Such a combination of elements yields an REB-heated fusion-electric propulsion system along the lines of Figure 1. This type of REB "electric arc" thruster is quite different from a conventional "hydrogen arcjet." In the latter, energy is added (inefficiently) to the propellant by ohmic resistive heating through the propellant gas/plasma. In the system of interest here, the propellant is heated (efficiently) by direct deposition of the REB beam energy into a central core of plasma, surrounded by centrifugally-radially-in-flowing propellant. Thermal radiation from this core is absorbed by the inflowing fluid/gas/plasma, which flows longitudinally along the system axis to the exit nozzle. The two keys to efficient heating are nearly complete absorption of thermal radiation in this process and nearly complete coupling of the REB into the central dense plasma. Beam/plasma coupling lengths must be small compared to the REB path through the thruster chamber.

Considerable study has been given to the unstable interaction of REBs with dense plasmas. The topic is too long to be treated here; however, results of this work[15] [16] [17] show that interaction lengths for e-folding energy deposition can be made as small as 10-20 cm, in plasmas at densities on the order of 10^{16}-10^{18} /cm^3. Thus, a thruster chamber length of 1-2 m will result in essentially complete beam absorption. Current filamentation can be suppressed by a longitudinal guide field supplied by magnet coils wound around the exterior surface. For example, a 250-G field will suffice for an REB carrying 1000 MWe at 500 keV and 2000 A distributed over a beam radius of 4 cm. Plasma temperatures up to the order of 10 eV (ca. 120,000 K) can be attained by this means.

The specific impulse that can be achieved with such plasma depends on the degree to which molecular dissociation and atomic ionization energy can be recovered in the nozzle flow. With hydrogen propellant, if none is

recovered, then I_{sp} = 8000 s; if all is recovered, then I_{sp} = 12,000 s. Of course, the essential element in this model of a fusion propulsion system is the fusion reactor. This must be based on the general inertial-electrostatic approach followed in the mid-1960s by Hirsch.[12] A new concept of electrostatic confinement exists and is under study[18] that may make this approach both feasible and practical. Detailed discussion of this concept is beyond the scope of this paper. If the direct-conversion process in the reactor can be made highly efficient, such a charged-particle-electric-discharge engine (called the QED engine) could, in principle, produce high thrust at high I_{sp}, with very small system mass. Superior vehicle performance then follows.
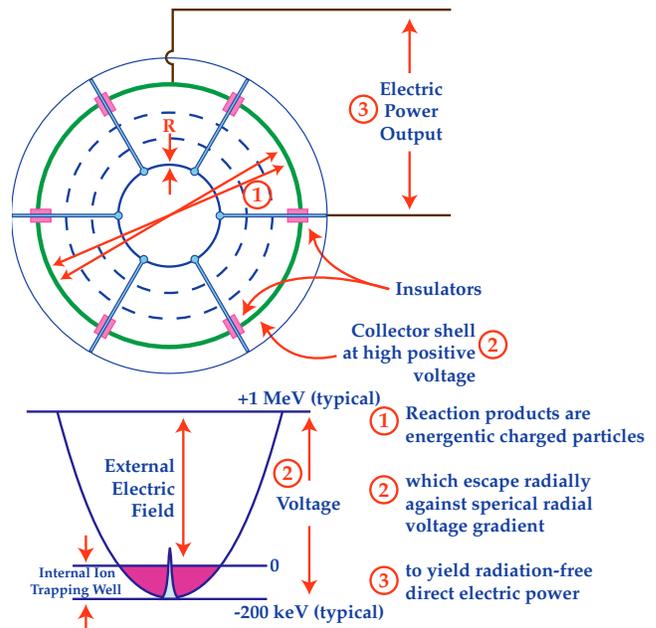

Figure 9 — Charged particle electric discharge (QED) fusion source with direct electrical conversion

As an example of this possibility, suppose that a QED engine system can be made with a specific mass of only a_{fes} = 5.0 x 10^{-3} kg/kW, that the waste-heat radiator operates at a temperature of T_r = 2000 K, radiates from one side only (b_{ij} = 1) with an emissivity of ε = 0.9, and that it has a mass co-efficient of a_{rad} = 20 kg/m^2. Furthermore, assume that a fusion electric gain of G_e = 50 can be achieved, so that the recirculating power fraction is only f_Q = 0.02. Further assume that f_L = 0.20 of the total fusion power is deposited directly in structure and that 0.20 of this (or 0.04 of total power) can be regeneratively cooled, while the rest (f_L =0.16) is rejected through the waste-heat radiator circuit. Taking the limiting regeneration temperature to be T_{reg} = 1800 K (2780°F), the upper limit value of I_{sp} can be shown to be about I_{sp} = 3100 s. The remaining 0.80 power fraction is converted directly to electricity (there is no thermal-electrical conversion process here) at an efficiency of n_{-c} = 0.95. The unconverted fraction (f_r = 0.04) of this power must also

be rejected by the waste-heat radiator. Thus, a fraction 0.04 of the total fusion power is cooled regeneratively, 0.20 is rejected in a high-temperature waste-heat radiator system, and 0.76 is electrical power which drives the REB plasma heater. The total power fraction going into the propellant stream is 0.80.

With these parameters, noting that $G_L = (1 - f_q)(G_e) = 49$ here, the system force acceleration can be calculated from Eq. 7 and corrected by a factor $(1 + P_{reg}/P_e)$ for the power regenerated into the propellant. Taking a degraded value of 3000 s for I_{sp}, the propulsion system force acceleration capability is then found to be $a_L = 0.55$ g_0. This level of performance would allow QED engine use for "high-thrust" rocket missions in near-Earth space or for winged, lifting aerospace-planes in single-stage-to-orbit flight.

Conclusions

Certain types of fusion power systems may offer superior space-flight performance, both in interplanetary and Earth/ moon space, if their specific mass can be made small enough. In the case of magnetic confinement of fusion fuels, it appears possible to achieve $a_L > 10^{-3}\ g_0$ by use of small, high-field, copper coil tokamaks operating on the DD reaction. Use of D^3He fuels could yield performance about two or three times higher than this.

Very much higher performance may be attained without neutron production, by use of the QED electric reactor concept for charged-particle reactions. If this concept proves feasible, a QED engine system could give performance two to three orders of magnitude better than that attainable from the small tokamak system. Typically, $a_L > 0.3\ g_0$, so that the QED system could be used for "high-thrust" Earth-related missions.

In either case, the flight performance of such fusion propulsion systems can be analyzed as though they were electrical propulsion systems with variable specific impulse from very high-gain engine thrusters.

Publication History

References

[1] Maxwell Hunter, "Solar System Spaceships," *Thrust Into Space*, Holt, Rhinehart, & Winston, New York, 1966, Chapter 5, p. 150.

[2] P.W. Garrison, and J. F. Stocky, "Future Spacecraft Propulsion," *Journal of Propulsion*, Volume 4, Number 6, 1988, pp. 520-525.

[3] F.G. Etheridge, "Solar Rocket Systems Concept Analysis," Air Force Astronautics Laboratory, Edwards Air Force Base, CA, AFRPL-TR-79-79, December 1979.

[4] Robert W. Bussard, and DeLauer, R. D., "Principles of Performance Analysis," *Fundamentals of Nuclear Flight*, McGraw-Hill, New York, 1965, Chapter 4, pp. 87-95.

[5] M. Auweter-Kurtz, H.L. Kurtz, and H.O. Schrade, "Optimization of Electric Propulsion Systems Considering Specific Power as Function of Specific Impulse," *Journal of Propulsion*, Volume 4, Number 6, 1988, pp. 512-519.

[6] Robert A. Gross, *Fusion Energy,* Wiley, New York, 1984, Chapters 7 and 8, pp. 184-266. ISBN 0-471-88470-7

[7] Robert W. Bussard, "Modular Fusion Reactor With Disposable Core," U.S. Patent No. 4,367,193, January 4, 1983.

[8] R.A. Jacobsen, C.E. Wagner, and R.E. Covert, "System Studies of High-Field Tokamak Ignition Experiments," *Journal of Fusion Energy*, Volume 3, Number 4, 1983.

[9] C.E. Wagner, "DD Riggatron Tokamaks," private communication, July 14, 1983.

[10] L.J. Wittenberg, J. F. Santarius, and G.L. Kulcinski, "Lunar Source of ^3He for Commercial Fusion Power," *Fusion Technology*, Volume 10, September 1986, pp. 167-178.

[11] William C. Elmore, James L. Tuck, and Kenneth M. Watson, "On the Inertial-Electrostatic Confinement of a Plasma," *Physics of Fluids*, Volume 2, May-June 1959, pp. 239-246.

[12] Robert L. Hirsch, "Inertial-Electrostatic Confinement of Ionized Fusion Gases," *Journal of Applied Physics*, Volume 38, Number 11, October 1967, pp. 4522-4534.

[13] Ralph W. Moir, and William L. Barr, "'Venetian Blind' Direct Energy Convertor for Fusion Reactors," *Nuclear Fusion*, Volume 13, 1973, p. 35.

[14] William L. Barr, and Ralph W. Moir, "Test Results on Plasma Direct Convertors," *Nuclear Technology and Fusion*, Volume 3, 1983, p. 98.

[15] Ronald C. Davidson, *Theory of Nonneutral Plasmas*, W.A. Benjamin, Inc., Reading, MA, 1974, pp. 83-85.

[16] Lester E. Thode, "Effect of Electron-Ion Collisions on the Nonlinear State of the Relativistic Two-Stream Instability," *Physics of Fluids*, Volume 20, No. 12, 1977, pp. 2121-2127. doi: 10.1063/1.861842

[17] David L. Book, *NRL Plasma Formulary,* revised edition, Laboratory for Computational Physics, Naval Research Laboratory, Washington, DC, 1983, pp. 46-50.

[18] Robert W. Bussard, G.P. Jellison, and G.E. McClellan, "Preliminary Research Studies of a New Method for Control of Charged Particle Interactions," Defense Nuclear Agency, PSR Report 1899, November 1988, Section I and Attachment A.